Original Article

DOI: 10.5582/bst.2012.v6.5.234

Density functional theory based quantitative structure-property relationship studies on coumarin-based prodrugs

Xinying Yang[1], Xuben Hou[1], Binghe Wang[1,2], Minyong Li[1,*], Hao Fang[1,*]

[1] *Department of Medicinal Chemistry, Key Laboratory of Chemical Biology (Ministry of Education), School of Pharmacy, Shandong University, Ji'nan, Shandong, China;*

[2] *Department of Chemistry and Center for Biotechnology and Drug Design, Georgia State University, Atlanta, GA, USA.*

Summary **A coumarin-based prodrug system plays a significant role in preparing esterase-sensitive prodrugs of amines and peptides. The electronic structures of 27 coumarin-based prodrugs developed in our lab were calculated at a B3LYP/6-31+G (d,p) level with a Gaussian 03 program. The calculated structural parameters were taken as theoretical descriptors to establish five novel QSPR models. The SMLR linear model (q^2 = 0.427, r^2 = 0.516) and the PLS linear model (q^2 = 0.584, r^2 = 0.663) were developed with descriptors selected by an Unsupervised Forward Selection method. Another three nonlinear QSPR models were established by a Polynomial Neural Network (PNN) Simulation method (q^2 = 0.692, 0.675, 0.663; r^2 = 0.700, 0.688, 0.672). We suggest that the QSPR models derived here, especially the PNN models, can be used to predict the release kinetics of coumarin-based prodrugs as well as design new derivatives of coumarin-based prodrug candidates.**

Keywords: Coumarin, prodrug, QSPR, quantitative structure-property relationship, DFT

1. Introduction

There is no doubt that prodrugs play an important role in current drug delivery and drug discovery (*1-3*). Our lab developed a coumarin-based prodrug system for preparing esterase-sensitive prodrugs of amines and peptides (*4*). This system has a *cis*-double bond which could facilitate the lactonization when an acyl group (R) is hydrolyzed by esterase (Scheme 1). To date, it has been used for the preparations of cyclic prodrugs of opioid peptides (*5-8*), such as DADLE (*9-11*) and DADLE analogs (*12*), and peptidomimetics, such as an RGD (Arg-Gly-Asp) analog MK-383 (*13,14*). Moreover, this system was also applied in the design of non-peptide prodrugs such as meptazinol, and the prodrug of meptazinol has shown a 4-fold increase in oral bioavailability (*15*). The advantage of the coumarin system lies in the released final product, coumarin, which is known to be non-toxic in extensive studies. In addition, the release rate of the coumarin-based prodrug system can be further manipulated by the introduction of additional substituents on the aromatic ring or the acyl group. In our previous studies, a series of coumarin derivatives with different substitutions of R and R_1-R_6 were synthesized and evaluated for release kinetics (Table 1) (*3,16-18*). These release kinetic studies only obtained overall pseudo-first-order rate constants because the complex process involves an enzymatic reaction and multi-step chemical reactions (Scheme 1). Our preliminary results suggest that the acyl group (R) has a minor influence on the overall half-lives, but the substituents on the phenyl ring (R_1-R_4) and amine part (R_5 and R_6) have major and complicated effects which include an electronic effect, steric effect and so on. In order to clearly illustrate these issues, computer-based tools are needed to further analyze the structural effect on the release kinetics.

Quantitative structure-property relationship (QSPR) studies have been successfully used for the prediction of physicochemical properties of chemical compounds based on their structures (*19-24*). The biological counterpart of such studies, quantitative

*Address correspondence to:
Dr. Fang Hao, Department of Medicinal Chemistry, School of Pharmacy, Shandong University, No. 44 Wenhua Road, Ji'nan, 250012, China.
E-mail: haofangcn@sdu.edu.cn
Dr. Minyong Li, Department of Medicinal Chemistry, School of Pharmacy, Shandong University, No. 44 Wenhua Road, Ji'nan, 250012, China.
E-mail: mli@sdu.edu.cn

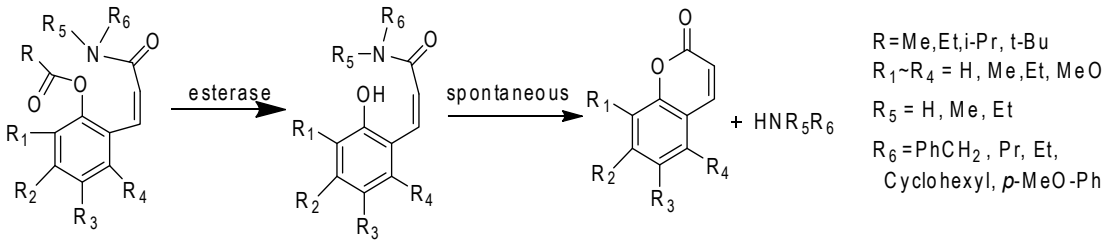

Scheme 1. The illustration of a coumarin-based esterase-sensitive prodrug system and its derivatives.

Tabel 1. The structure of coumarin derivatives

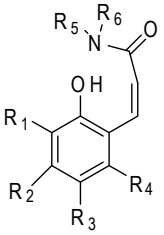

Compound	R1	R2	R3	R4	R5	R6
1	H	H	H	H	H	Benzyl
2	H	H	H	H	H	Benzyl
3	H	H	H	H	H	Benzyl
4	H	H	H	H	H	Benzyl
5	H	H	H	H	H	Pr
6	H	H	H	H	H	Cyclohexyl
7	H	H	H	H	H	p-MeO-Ph
8	H	H	H	H	Me	Benzyl
9	H	H	H	H	Et-	Et
10	Me	H	H	Me	Me	Benzyl
11	Me	H	H	Me	Et	Et
12	H	Me	H	Me	Me	Benzyl
13	H	Me	H	Me	Et	Et
14	Me	Me	H	H	Me	Benzyl
15	Me	Me	H	H	Et	Et
16	Me	H	Me	H	Me	Benzyl
17	Me	H	Me	H	Et	Et
18	Me	H	H	H	Me	Benzyl
19	Me	H	H	H	Et	Et
20	H	Me	Me	Me	Me	Benzyl
21	H	Me	Me	Me	Et	Et
22	H	H	Me	H	Me	Benzyl
23	H	H	Me	H	Et	Et
24	H	Me	H	H	Me	Benzyl
25	H	Me	H	H	Et	Et
26	H	MeO	H	H	Me	Benzyl
27	H	MeO	H	H	Et	Et

structure-activity relationships (QSAR), has also been extensively used with great success *(25-28)*. So far, many efforts have successfully been made to investigate the spectral properties by using this kind of QSAR/QSPR approach (*29-31*). However, a common problem in QSAR/QSPR modeling is choosing a proper description of the variance between the individual molecular structures within a set of compounds. In our case, some commercially available 3D-QSAR methods, such as CoMFA and CoMSIA, cannot be used in such a complex system because these approaches mainly focus on interaction between macromolecules (receptors, enzymes) and substrates, while the kinetics of the coumarin-based prodrug system is more complicated and consists of not only the enzyme hydrolysis interaction but also intramolecular lactonization steps. The latter lactonization step is also significantly different from molecular recognition in biological systems. Currently, quantum-mechanical descriptors calculated using density functional theory (DFT) have been successfully used in the modeling of reaction-related procedures, such as free-radical copolymerization (*32*), bond dissociation (*33*), and olefin metathesis (*34*). Therefore, the structure parameters of the coumarin-based prodrug, especially the parameters related to the lactonization step should be taken into account due to the chemical reactivity of bond making and bond breaking. In this paper, we will use the DFT-based QSPR computational tool and statistics method to study the relationships between the coumarin-based prodrug system and their kinetics.

2. Materials and Methods

2.1. *DFT calculations*

Electronic structure calculations have been performed using the Gaussian 03 program (*35*) on URSA, a 160-processor computer based on the Power5+ processor and IBM's P series architecture. The DFT method B3LYP (*36,37*) and the 6-31+G (d,p) basis set were used for all calculations, along with the PCM solvation model (*38*). The PCM solvation model is used in single-point energy calculations (PCM (sp)), and during the geometry optimizations and frequency calculations (PCM (opt)). All calculations using the PCM solvent model employ UAHF atomic radii when constructing the solvent cavity, as recommended in the Gaussian 03 user's reference when the "scfvac" keyword is used to obtain the free energy of solvation, as is the case in this study. All the geometries are fully optimized, and the character of the stationary points found is confirmed by a harmonic frequency calculation at the same theory level to ensure a minimum is located. Such a practice is also the same as we have done in past studies (*39,40*). The kinetic constants and all structure parameters related to enzyme hydrolysis interaction and intramolecular lactonization of each compound are listed in Table 2.

Table 2. Structure parameters of coumarin derivatives based on DFT calculations

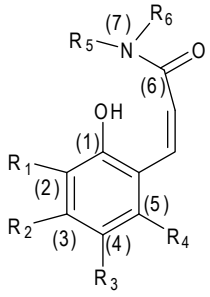

No.	X1	X2	X3	X4	X5	X6	X7	X8	X9	X10	X11	X12	X13	X14	X15	X16	X17	Y
1	−11.28	−18.06	33.75	−34.77	7.80	6.78	3.84	5.92	−0.353	−0.571	0.263	−0.328	−0.148	−0.441	−0.707	−0.194	58.02	4.86
2	−11.24	−17.96	33.73	−34.82	7.80	6.72	3.75	5.80	−0.350	−0.571	0.261	−0.330	−0.149	−0.434	−0.715	−0.191	61.16	4.81
3	−11.22	−17.95	33.74	−34.81	7.80	6.73	3.77	5.82	−0.353	−0.571	0.261	−0.328	−0.154	−0.430	−0.723	−0.191	61.04	4.76
4	−11.23	−17.96	33.73	−34.80	7.81	6.74	3.77	5.83	−0.345	−0.570	0.259	−0.329	−0.148	−0.431	−0.719	−0.191	61.14	4.76
5	−7.67	−14.42	29.30	−28.13	5.56	6.74	4.27	5.71	0.088	−0.546	−0.164	−0.232	−0.122	−0.374	−0.033	−0.287	45.05	4.97
6	−10.81	−16.87	32.15	−32.89	6.81	6.07	3.52	4.66	−0.429	−0.529	0.238	−0.356	−0.065	−0.397	−0.040	−0.329	49.87	4.36
7	−9.43	−16.58	34.96	−34.19	6.38	7.15	5.11	7.04	−0.267	−0.544	0.056	−0.358	0.066	−0.468	−0.224	−0.322	57.13	5.72
8	−7.93	−16.47	35.39	−34.42	7.57	8.54	2.72	3.76	−0.266	−0.564	0.272	−0.411	−0.167	−0.192	−0.349	−0.067	55.55	4.55
9	−8.05	−14.61	30.70	−30.47	6.33	6.56	2.81	3.97	−0.153	−0.560	0.198	−0.221	−0.291	−0.123	−0.375	−0.010	53.60	3.79
10	−5.14	−14.75	39.58	−37.74	7.77	9.61	2.58	3.56	0.404	−0.504	1.002	−0.767	0.273	0.064	−0.624	−0.036	70.12	5.15
11	−2.36	−9.15	33.91	−33.60	6.47	6.78	5.09	7.24	0.002	−0.594	1.191	−0.770	−0.124	0.585	−0.375	−0.058	60.12	5.01
12	−5.31	−15.71	39.56	−37.27	8.10	10.40	2.64	3.66	0.079	−0.521	0.097	0.226	−0.126	0.348	−0.354	−0.070	61.93	5.26
13	−6.08	−13.67	34.98	−34.07	6.69	7.60	3.03	4.30	0.232	−0.518	−0.280	0.239	0.305	0.052	−0.366	−0.006	61.52	4.79
14	−4.53	−14.87	39.38	−36.24	7.20	10.34	3.49	4.63	0.029	−0.493	−0.126	0.543	−0.268	−0.079	−0.466	0.005	64.87	5.56
15	−6.01	−13.20	34.86	−34.23	6.56	7.19	2.75	3.80	0.187	−0.522	0.878	0.139	−0.767	0.184	−0.469	0.011	57.31	4.99
16	−5.74	−14.95	39.78	−38.10	7.53	9.22	2.73	3.50	−0.473	−0.565	1.269	−1.240	0.733	−0.653	−0.670	−0.037	77.09	5.14
17	−4.91	−12.82	35.01	−33.49	6.39	7.91	2.88	4.11	−0.954	−0.522	0.970	−0.533	−0.022	0.836	−0.449	−0.012	58.25	4.40
18	−4.86	−14.60	37.37	−34.67	7.04	9.74	3.77	4.89	0.271	−0.515	0.124	−0.050	−0.430	−0.006	−0.134	−0.039	64.68	5.20
19	−5.88	−12.90	32.96	−32.24	6.29	7.01	2.43	3.52	−0.193	−0.550	0.943	−0.678	−0.237	−0.016	−0.447	0.005	55.02	4.58
20	−4.71	−15.71	41.38	−38.57	8.19	10.99	2.91	4.04	−0.242	−0.512	−0.142	0.512	0.064	0.680	−0.411	−0.051	70.81	5.09
21	−6.02	−13.74	36.53	−35.67	6.85	7.71	3.28	4.66	−0.112	−0.508	−0.091	0.712	−0.084	0.438	−0.434	−0.028	68.56	4.40
22	−7.35	−16.52	37.11	−35.66	7.72	9.17	2.95	4.13	−0.209	−0.569	0.291	−0.558	0.440	−0.375	−0.433	−0.061	54.45	4.63
23	−7.19	−14.55	32.74	−31.84	6.47	7.37	3.18	4.46	−0.170	−0.572	0.264	−0.722	0.461	−0.329	−0.410	−0.040	50.68	3.76
24	−7.37	−16.51	37.57	−36.34	7.92	9.15	2.91	3.94	−0.093	−0.565	0.481	−0.024	−0.714	0.120	−0.398	−0.060	58.73	4.56
25	−7.91	−14.80	32.94	−32.78	6.73	6.89	2.85	3.97	−0.031	−0.565	−0.144	0.300	−0.415	0.211	−0.478	0.002	52.46	3.72
26	−9.29	−18.43	38.82	−37.66	7.98	9.13	2.74	3.37	−0.541	−0.571	1.000	−0.515	−0.492	−0.018	−0.371	−0.072	65.78	4.52
27	−9.22	−15.99	34.30	−34.25	6.72	6.77	3.68	5.24	−0.133	−0.558	0.109	−0.269	0.243	−0.387	−0.473	−0.031	61.87	3.76

Y: logK (*10^4/s), represent the observed release kinetic value (k_{obs}) of coumarin-based prodrugs; X1: ΔG(kcal/mol), X2: Total electrostatic energy (kcal/mol), X3: Cavitation energy (kcal/mol), X4: Dispersion energy (kcal/mol), X5: Repulsion energy (kcal), X6: Total non electrostatic energy (kcal/mol), X7: dipole in vacuo (Debye), X8: dipole in solution (Debye), X9: atomic Mulliken charge of atom C(1), X10: atomic Mulliken charge of O(1), X11: atomic Mulliken charge of C(2), X12: atomic Mulliken charge of C(3), X13: atomic Mulliken charge of C(4), X14: atomic Mulliken charge of C(5), X15: atomic Mulliken charge of C(6), X16: atomic Mulliken charge of N(7), X17: surface of added spheres.

2.2. *Rational selection of descriptors*

After identification of a large number of descriptors, a rational descriptor selection was carried out to reduce the number of descriptors to an acceptable level containing no redundancy and a minimal amount of multicollinearity. In this selection, a novel descriptor reduction algorithm, unsupervised forward selection (UFS) (*41*), was employed to determine suitable descriptors. This method has been successfully used in our previousstudy for modeling the excitation wavelengths of boronic acids (*42*). UFS could select from a data matrix a maximal linearly independent set of columns with a minimal amount of multiple correlations, and therefore it was designed for use in the development of QSPR models, where the *m* by *n* data matrix contains the values of *n* variables (typically molecular properties) for *m* objects (typically compounds). In the descriptor selection, variables with small variance (not significant at the 5% level) were then removed. The UFS procedure was then applied repeatedly using values of R^2_{max} stepping from 0.1 to 0.9 with an increment of 0.1, together with R^2_{max} = 0.99. The UFS calculation was performed on a Virtual Computational Chemistry Laboratory at *http://www.vcclab.org* (*43*).

2.3. *Polynomial neural network (PNN) simulation*

The PNN algorithm is also known as an iterational algorithm of group methods of data handling (GMDH) (*44*). PNN provides a robust nonlinear polynomial regression identification for numerical data with unknown dependencies (*45*). Moreover it is insensible to outliers and irrelevant variables, and provides fast learning and numerical stability. PNN is a robust

Table 3. Three neural network models and statistical data

Model	Equation	q^2	r^2	RMSE	F	MAE
SMLR	Y = 0.286 × X6 + 0.312 × X8 + 0.984	0.427	0.516	0.380	26.60	--
PLS	Y = 0.164 × X6 + 0.121 × X8 + 0.423 × X9 + 7.088 × X10 + 0.066 × X15 - 1.269 × X16 + 6.697	0.584	0.663	0.310	49.08	--
PNN 1	Y = 5.31 × X14 × X16 + 0.381 × $(X11)^2$ + 0.293 × X8 + 0.387 × X6	0.692	0.700	0.291	58.10	0.204
PNN 2	Y = 7.07 × $(X16)^2$ - 0.762 × X11 × X15 + 0.375 × X6 + 0.313 × X8	0.675	0.688	0.299	54.67	0.207
PNN 3	Y = 4.31 × X14 × X16 - 0.667 × X11 × X15 + 0.311 × X8 + 0.381 × X6	0.663	0.672	0.304	51.10	0.211

method that can be used even in the presence of outliers in the training set and provides reliable results even for such difficult cases. PNN correlates input and target variables using (non) linear regression. The PNN simulation was performed on a Virtual Computational Chemistry Laboratory at *http://www.vcclab.org* (*43*).

3. Results

3.1. *Selection of descriptors*

In the first step, UFS was used to optimize the number of descriptors. After UFS, only 11 descriptors, X4, X6, X8, X9, X10, X11, X13, X14, X15, X16, and X17, were significantly correlated with Y at a 95% level among all descriptors. These 11 descriptors were then used as input for the development of the linear and nonlinear QSPR models of coumarin-based prodrug. The UFS selected descriptors, classes and references are shown in Table 1.

3.2. *SMLR linear model*

Based on these 11 descriptors after selection, 27 compounds were then used to develop an optimal SMLR linear model. For the development of the linear model, leave-one-out (LOO) cross-validation statistical parameters were calculated to evaluate the model quality. Finally, a two-descriptor (X6 and X8) correlation model was obtained as represented in Table 3. The obtained squared correlation (r^2) was 0.516 and the LOO squared correlation (q^2) was 0.427. The standard error (RMSE) was 0.38 and the *F*-value was 26.60. The estimated values based on the SMLR linear model are listed in Table 4. Figure 1 depicts the estimated *versus* experimental values for all compounds.

3.3. *PLS linear model*

The linear model was also developed by PLS using 11 selected descriptors. In this case a correlation model including six descriptors, X6, X8, X9, X10, X15, and X16, was obtained as shown in Table 3. The number of PLS components is 3. In this linear model, r^2 was 0.663 and q^2 was 0.584. RMSE was 0.310 and the *F*-value was 49.68. The estimated results of the PLS model are shown in Table 4. The experimental and estimated values are shown in Figure 1.

Table 4. Experimental *versus* estimated data

No.	Experimental	SMLR	PLS	PNN		
				Model 1	Model 2	Model 3
1	4.86	4.77	4.88	4.84	4.81	4.91
2	4.81	4.71	4.84	4.77	4.74	4.84
3	4.76	4.72	4.85	4.77	4.75	4.85
4	4.76	4.73	4.86	4.78	4.75	4.86
5	4.97	4.69	4.88	4.86	4.89	4.80
6	4.36	4.17	4.55	4.43	4.51	4.33
7	5.72	5.22	5.37	5.63	5.63	5.57
8	4.55	4.59	4.43	4.50	4.49	4.54
9	3.79	4.09	3.95	3.72	3.76	3.79
10	5.15	4.84	5.30	5.13	5.21	5.17
11	5.01	5.18	4.63	5.10	5.17	4.98
12	5.26	5.10	5.22	4.97	5.11	5.02
13	4.79	4.49	4.62	4.23	4.12	4.16
14	5.56	5.38	5.49	5.36	5.29	5.34
15	4.99	4.22	4.40	4.20	4.20	4.20
16	5.14	4.71	4.61	5.34	5.21	5.27
17	4.40	4.52	4.37	4.57	4.59	4.54
18	5.20	5.29	5.22	5.21	5.21	5.24
19	4.58	4.08	4.02	4.08	4.05	4.04
20	5.09	5.38	5.41	5.26	5.36	5.25
21	4.40	4.64	4.78	4.29	4.33	4.30
22	4.63	4.89	4.68	4.91	4.86	4.96
23	3.76	4.48	4.25	4.26	4.26	4.32
24	4.56	4.83	4.67	4.75	4.84	4.81
25	3.72	4.19	4.07	3.84	3.78	3.81
26	4.52	4.64	4.39	4.91	4.80	4.78
27	3.76	4.55	4.39	4.22	4.23	4.29

3.4. *PNN simulation of QSPR*

In this case a nonlinear PNN model of QSPR was developed with the same selected subset of 6 descriptors from those linear models. The estimated results of the PNN model are given in Table 4. Figure 1 represents the estimated *versus* experimental values using the PNN nonlinear model.

3.5. *Interpretation of descriptors*

From Table 4, descriptors X3, X9, X15, and X16 existed in the three PNN non-linear models. Descriptors X5 and X12 showed their influence on PNN model 3 and model 1 respectively. Both the cavitation energy (X3) and repulsion energy (X5) belong to the components of free energy of solvation. Cavitation energy described the energy required to push aside the solvent molecules and then making a cavity to place a

solute molecule. Repulsion energy (X5) reflects the Van *der Walls* effect on solvation.

4. Discussion

To discuss the descriptors X9, X12, X15, and X16 in the PNN models, it is necessary to illustrate the mechanism of the coumarin-based esterase sensitive prodrug systems (Scheme 2). It was reported that the acyl group R of 28 would be easily hydrolyzed by esterase at physiological pH and generate 29 with an unmasked phenol group. Due to the *cis*-geometry of the double bond in the structure of 29, the spontaneous lactonization was easily triggered by the phenolic hydroxyl group attacking the carbonyl group of C-6 to form the tetrahedral 30. Then, the collapse of tetrahedral 30 would yield *cis*-coumarinic acid 31 and amine (*3*).

According to the mechanism of the coumarin-based prodrug, the carbonyl of C-1 would be hydrolyzed by esterase and the positive charge in C-1 will benefit hydrolysis of the acyl group. Therefore, the atomic charge of C-1 (X9) should have an influence on the release kinetics of the coumarin prodrug system. In addition, considering the carbonyl group of the amide at C-6 would be attacked by the unmasked phenolic hydroxyl group in the lactonization step of 29, the positive atomic charge in C-6 (X15) should no doubt lead to enhance the release kinetics of the coumarin prodrug syetem for the same reason. Then, the atomic charge on C-3 (X12) only existed in model 1, which perhaps exerts an effect on the unmasked phenolic hydroxyl group with an inductive or conjugated effect. It was reported that stabilizing a developing negative charge on the nitrogen (N-1) would facilitate lactonization during the collapse of the tetrahedral intermediate 30 (*3*). Furthermore, the nitrogen charges also related to the *pKa* value of the amine which could affect the release rate of the coumarin system in our preliminary study. Therefore, the atomic charge of nitrogen (X16) is an important descriptor in three models of PNN.

In conclusion, the present report demonstrates that DFT-based QSPR models can be used successfully to predict the release kinetics of the coumarin-based prodrug system. Among these models, the nonlinear

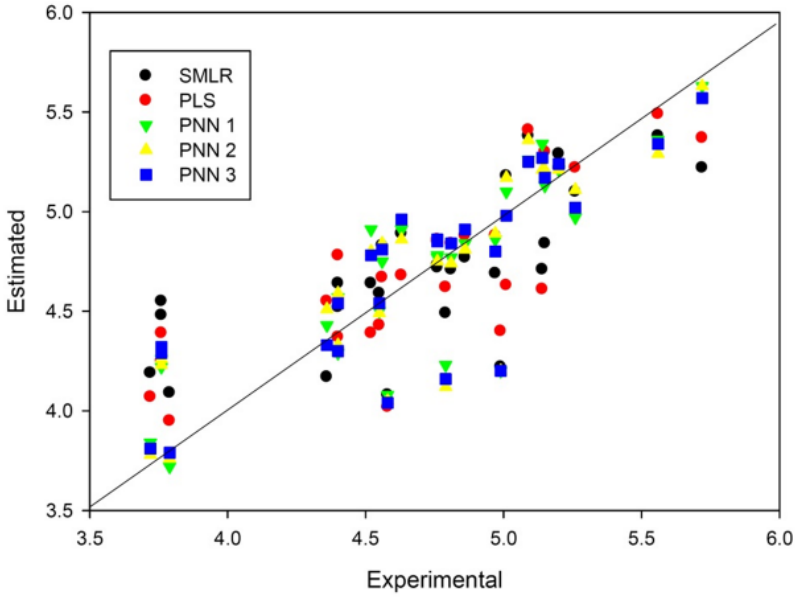

Figure 1. Estimated *versus* experimental values using three different models.

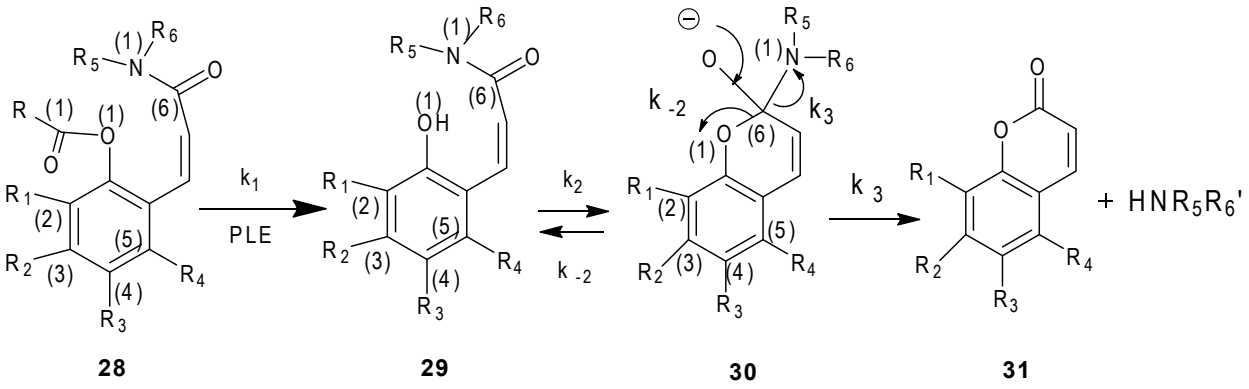

Scheme 2. The mechanism of the coumarin-based esterase sensitive prodrug system.

PNN models can provide estimated results in good agreement with experimental values. The descriptor of atomic charge of C-1, C-6 and N-1 exhibited more contributions to the prodrug release rate. In summary, this DFT-based QSPR approach can be a convenient way to predict release kinetics of coumarin prodrugs and the relative descriptors can also contribute to exploration of new derivatives of coumarin-based prodrug candidates.

Acknowledgements

This work was supported by a grant from NIH under Grant P20 GM065762 in USA, Scientific Research Foundation for Returned Overseas Chinese Scholars, State Education Ministry and Independent Innovation Foundation of Shandong University (IIFSDU, Grant No. 2012JC003) in China.

References

1. Huttunen KM, Rautio J. Prodrugs – an efficient way to breach delivery and targeting barriers. Curr Top Med Chem. 2011; 11:2265-2287.
2. Barot M, Bagui M, Gokulgandhi MR, Mitra AK. Prodrug strategies in ocular drug delivery. Med Chem. 2012; 8:753-768.
3. Fang H, Kaur G, Wang B. Functional Group Approaches to Prodrugs: Functional Groups in Peptides. In Prodrugs: Challenges and Rewards Part 2, Volume 5 (Stella VJ, Borchardt RT, Hageman MJ, Oliyai R, Tilley J, eds.). Springer, Berlin, German, 2007.
4. Wang B, Zhang H, Wang W. Chemical feasibility studies of a potential coumarin-based prodrug system. Bioorg Med Chem Lett. 1996; 6:945-950.
5. Gudmundsson OS, Jois SD, Vander Velde DG, Siahaan TJ, Wang B, Borchardt RT. The effect of conformation on the membrane permeation of coumarinic acid- and phenylpropionic acid-based cyclic prodrugs of opioid peptides. J Pept Res. 1999;53:383-392.
6. Gudmundsson OS, Pauletti GM, Wang W, Shan D, Zhang H, Wang B, Borchardt RT. Coumarinic acid-based cyclic prodrugs of opioid peptides that exhibit metabolic stability to peptidases and excellent cellular permeability. Pharm Res. 1999; 16:7-15.
7. Zych LA, Yang WQ, Liao Y, Griffin KR, Wang B. The effect of substitution patterns on the release rates of opioid peptides DADLE and [Leu(5)]-enkephalin from coumarin prodrug moieties. Bioorg Chem. 2004; 32:109-123.
8. Wang B, Siahaan T, Soltero R. Drug Delivery: Principles and Applications. John Wiley & Sons, Inc., New York City, NY, USA, 2005.
9. Ouyang H, Andersen TE, Chen W, Nofsinger R, Steffansen B, Borchardt RT. A comparison of the effects of p-glycoprotein inhibitors on the blood-brain barrier permeation of cyclic prodrugs of an opioid peptide (DADLE). J Pharm Sci. 2009; 98:2227-2236.
10. Tang F, Borchardt RT. Characterization of the efflux transporter(s) responsible for restricting intestinal mucosa permeation of the coumarinic acid-based cyclic prodrug of the opioid peptide DADLE. Pharm Res. 2002; 19:787-793.
11. Zych LA, Yang W, Liao Y, Griffin KR, Wang B. The effect of substitution patterns on the release rates of opioid peptides DADLE and [Leu(5)]-enkephalin from coumarin prodrug moieties. Bioorg Chem. 2004; 32:109-123.
12. Nofsinger R, Fuchs-Knotts T, Borchardt RT. Factors that restrict the cell permeation of cyclic prodrugs of an opioid peptide, part 3: Synthesis of analogs designed to have improved stability to oxidative metabolism. J Pharm Sci. 2012; 101:3486-3499.
13. Wang W, Jiang J, Ballard CE, Wang B. Prodrug approaches to the improved delivery of peptide drugs. Curr Pharm Des. 1999; 5:265-287.
14. Wang W, Camenisch G, Sane DC, Zhang H, Hugger E, Wheeler GL, Borchardt RT, Wang B. A coumarin-based prodrug strategy to improve the oral absorption of RGD peptidomimetics. J Control Release. 2000; 65:245-251.
15. Xie Q, Wang X, Wang X, Jiang Z, Qiu Z. Design, synthesis, and bioavailability evaluation of coumarin-based prodrug of meptazinol. Bioorg Med Chem Lett. 2005; 15:4953-4956.
16. Liao Y, Hendrata S, Bae SY, Wang B. The effect of phenyl substituents on the release rates of esterase-sensitive coumarin-based prodrugs. Chem Pharm Bull (Tokyo). 2000; 48:1138-1147.
17. Liao Y, Wang B. Substituted coumarins as esterase-sensitive prodrug moieties with improved release rates. Bioorg Med Chem Lett. 1999; 9:1795-1800.
18. Wang B, Wang W, Camenisch GP, Elmo J, Zhang H, Borchardt RT. nthesis and evaluation of novel coumarin-based esterase-sensitive cyclic prodrugs of peptidomimetic RGD analogs with improved membrane permeability. Chem Pharm Bull (Tokyo). 1999; 47:90-95.
19. Jorgensen WL. QSAR/QSPR and proprietary data. J Chem Inf Model. 2006; 46:937.
20. Dyekjaer JD, Jonsdottir SO. QSPR models for various physical properties of carbohydrates based on molecular mechanics and quantum chemical calculations. Carbohydr Res. 2004; 339:269-280.
21. Fayet G, Rotureau P, Joubert L, Adamo C. Development of a QSPR model for predicting thermal stabilities of nitroaromatic compounds taking into account their decomposition mechanisms. J Mol Model. 2011; 17:2443-2453.
22. Katritzky AR, Stoyanova-Slavova IB, Tämm K, Tamm T, Karelson M. Application of the QSPR approach to the boiling points of azeotropes. J Phys Chem A. 2011; 115:3475-3479.
23. Peng S, Jian-Wei Z, Peng Z, Lin X. QSPR modeling of bioconcentration factor of nonionic compounds using Gaussian processes and theoretical descriptors derived from electrostatic potentials on molecular surface. Chemosphere. 2011; 83:1045-1052.
24. Zeng XL, Wang HJ, Wang Y. QSPR models of n-octanol/water partition coefficients and aqueous solubility of halogenated methyl-phenyl ethers by DFT method. Chemosphere. 2012; 86:619-625.
25. Selassie CD, Mekapati SB, Verma RP. QSAR: Then and now. Curr Top Med Chem. 2002; 2:1357-1379.
26. Brown N, Lewis RA. Exploiting QSAR methods in lead optimization. Curr Opin Drug Discov Devel. 2006; 9:419-424.
27. Hou X, Du J, Fang H, Li M. 3D-QSAR study on a series of Bcl-2 protein inhibitors using comparative molecular

field analysis. Protein Pept Lett. 2011; 18:440-449.
28. Zhang L, Fang H, Zhu HW, Wang Q, Xu WF. QSAR studies of histone deacetylase (HDAC) inhibitors by CoMFA, CoMSIA, and molecular docking. Drug Discov Ther. 2009; 3:41-48.
29. Hui-Ying X, Jian-Wei Z, Gui-Xiang H, Wei W. QSPR/QSAR models for prediction of the physico-chemical properties and biological activity of polychlorinated diphenyl ethers (PCDEs). Chemosphere. 2010; 80:665-670.
30. Mercader AG, Duchowicz PR, Fernandez FM, Castro EA. Replacement method and enhanced replacement method *versus* the genetic algorithm approach for the selection of molecular descriptors in QSPR/QSAR theories. J Chem Inf Model. 2010; 50:1542-1548.
31. Rayne S. Comment on "QSPR/QSAR models for prediction of the physicochemical properties and biological activity of polybrominated diphenyl ethers" by X. Hui-Ying, Z. Jian-Wei, Y. Qing-Sen, W. Yan-Hua, Z. Jian-Ying, and J. Hai-Xiao" [Chemosphere 66 (10) (2007) 1998-2010]. Chemosphere. 2010; 81:553.
32. Yu X, Liu W, Liu F, Wang X. DFT-based theoretical QSPR models of Q-e parameters for the prediction of reactivity in free-radical copolymerizations. J Mol Model. 2008; 14:1065-1070.
33. Bosque R, Sales J. A QSPR study of O-H bond dissociation energy in phenols. J Chem Inf Comput Sci. 2003; 43:637-642.
34. Occhipinti G, Bjorsvik HR, Jensen VR. Quantitative structure-activity relationships of ruthenium catalysts for olefin metathesis. J Am Chem Soc. 2006; 128:6952-6964.
35. M. J. Frisch, G. W. Trucks, H. B. Schlegel, *et al*. Gaussian 03, Revision C.02. Volume 24. Wallingford CT: Gaussian, Inc., Pittsburgh, PA, USA, 2004.
36. Axel DB. Density-functional thermochemistry. III. The role of exact exchange. J Chem Phys. 1993; 98:5648-5652.
37. Lee C, Yang W, Parr RG. Development of the Colle-Salvetti correlation-energy formula into a functional of the electron density. Phys Rev B. 1988; 37:785.
38. Cances E, Mennucci B, Tomasi J. A new integral equation formalism for the polarizable continuum model: Theoretical background and applications to isotropic and anisotropic dielectrics. J Chem Phys. 1997; 107:3032-3041.
39. Jin S, Wang J, Li M, Wang B. Synthesis, evaluation, and computational studies of naphthalimide-based long-wavelength fluorescent boronic Acid reporters. Chem Eur J. 2008; 14:2795-2804.
40. Jin S, Li M, Zhu C, Tran V, Wang B. Computer-based *de novo* design, synthesis, and evaluation of boronic acid-based artificial receptors for selective recognition of dopamine. Chembiochem. 2008; 9:1431-1438.
41. Whitley DC, Ford MG, Livingstone DJ. Unsupervised forward selection: A method for eliminating redundant variables. J Chem Inf Comput Sci. 2000; 40:1160-1168.
42. Li M, Ni N, Wang B, Zhang Y. Modeling the excitation wavelengths (lambda(ex)) of boronic acids. J Mol Model. 2008; 14:441-449.
43. Tetko IV, Gasteiger J, Todeschini R, Mauri A, Livingstone D, Ertl P, Palyulin VA, Radchenko EV, Zefirov NS, Makarenko AS, Tanchuk VY, Prokopenko VV. Virtual computational chemistry laboratory – design and description. J Comput Aided Mol Des. 2005; 19:453-463.
44. Tetko IV, Aksenova TI, Volkovich VV, Kasheva TN, Filipov DV, Welsh WJ, Livingstone DJ, Villa AEP. Polynomial neural network for linear and non-linear model selection in quantitative-structure activity relationship studies on the internet. SAR QSAR Environ Res. 2000; 11:263-280.
45. Aksyonova TI, Volkovich VV, Tetko IV. Robust polynomial neural networks in quantative-structure activity relationship studies. Syst Anal Model Simul. 2003; 43:1331-1339.

(*Received August 13, 2012; Revised September 20, 2012; Accepted September 24, 2012*)